AIAA JOURNAL
Vol. 37, No. 12, December 1999

Inverse Design Optimization of Transonic Wings Based on Multi-Objective Genetic Algorithms

Shinichi Takahashi,* Shigeru Obayashi,† and Kazuhiro Nakahashi‡
Tohoku University, Sendai 980-8579, Japan

Multi-objective genetic algorithms (MOGAs) have been applied to optimize an inverse design of a transonic wing shape. First, the wing planform is optimized by solving a multidisciplinary optimization problem based on aerodynamic, structural, and fuel storing objectives and constraints. Second, three-dimensional target pressure distribution is optimized for the aerodynamic inverse design with the previously designed planform. Minimization of the profile drag and the induced drag is performed under constraints on lift and other design principles. Applying these two preprocessing procedures by using MOGAs, Pareto surfaces can be studied for tradeoffs among multiple objectives. Thus, a designer is able to choose a good compromise for wing planform and target pressures for the inverse design. Corresponding for wing surface geometry is obtained by Takanashi's inverse method, and a sample design result is given.

Introduction

THERE is a long history for flow control and optimization in human civilization. Gunzburger introduced an interesting viewpoint in a history.[1] From his discussions, approaches taken in this area may be categorized in three ways: 1) flow optimization without sophisticated flow equations, 2) flow optimization without sophisticated optimization techniques, and 3) flow optimization with sophisticated flow equations and optimization techniques.

An example of the first category, flow optimization without sophisticated flow equations, is aerodynamic controls. A desired aircraft maneuver is obtained by controlling a position of the rudder, elevators, ailerons, and so on. Aerodynamic controls are determined by solving ordinary differential equations where the influence of the flow appears as functions or constants. These functions and constants are given a priori, and no attempt is made to solve the governing partial differential equations of fluid motions.

Design of transonic shock-free airfoils gives a good example of the second category, flow optimization without sophisticated optimization techniques. Absence of the shock wave is first considered as an indication of the global minimum for the wave drag. Then, an airfoil shape that generates a shock-free flow is sought. Typical shock-free airfoils have been found by analysis based on the flow physics, not by optimization techniques.

The third approach that combines sophisticated flow equations and optimization techniques is now of strong interest in the field of aerospace engineering. Good reviews for flow optimization techniques based on the adjoint formulation are found in Refs. 2 and 3. The adjoint approach will be an efficient aerodynamic design optimization tool, but it inherits a limitation of the gradient-based search. It naturally assumes the aerodynamic objectives are smooth. As reported in Refs. 4 and 5, however, they are not necessarily smooth.

An alternative strategy for aerodynamic design is the inverse design approach.[6] Inverse methods seek a geometry that yields a prescribed pressure distribution by using an iterative modification to the boundary shape. Specification of target pressures is dictated by the flow physics. Therefore, the inverse design approach falls into the third category, flow optimization without sophisticated optimization techniques. In other words, the inverse design method gives an optimal design only if a designer is able to specify an optimal target pressure.

Although experienced designers are capable of translating their design goals into properly defined pressure distributions in the inverse design approach, the requirement for experiences often becomes an obstacle in real-world applications. To address this problem, optimization of target pressures for transonic airfoils was discussed in Refs. 7 and 8. The inverse method following the optimization of target pressures forms a unique hybrid approach for the flow optimization.

This paper deals with an extension of this hybrid approach to three dimensions. Suppose x is the chordwise direction, z is the airfoil contour, and p is the corresponding pressure. The inverse method can be described as follows: Specify $p_{\text{target}}(x)$, then obtain $z(x)$ so that $p(x) = p_{\text{target}}(x)$ for $0 \le x \le c$, where c is a chord length. The inverse optimization method can be written as follows: Optimize $p_{\text{target}}(x)$, then obtain $z(x)$ so that $p(x) = p_{\text{target}}(x)$ for $0 \le x \le c$. This statement can be extended to three dimensions by using the spanwise direction y as follows: Optimize $p_{\text{target}}(x, y)$, then obtain $z(x, y)$ so that $p(x, y) = p_{\text{target}}(x, y)$.

To execute this, however, ranges of x and y, that is, wing planform, should be specified and optimized as well. Therefore, this paper considers two optimization problems: wing planform optimization and three-dimensional target pressure optimization. These two optimization steps are preprocesses for the inverse design. The final wing geometry will be obtained by executing the inverse design. The resulting steps can be summarized as follows: First optimize planform(x, y), then optimize $p_{\text{target}}(x, y)$, finally obtain $z(x, y)$ so that $p(x, y) = p_{\text{target}}(x, y)$.

In standard aircraft design procedure, the wing planform shape has to be determined at an early stage of aircraft design because the planform shape is closely related to aircraft sizing. In this stage, designers should account for tradeoff information between aerodynamic performance, structural strength, and weight, fuel storage, and so on. Therefore, an automated design of the wing planform shape requires multidisciplinary design optimization (MDO) based on a system composed of aerodynamics, structural dynamics, etc. This naturally decouples the wing planform optimization from the target pressure optimization because the latter is a purely aerodynamic problem.

The MDO problem for the wing planform design was extensively investigated in Ref. 9 by using a standard optimization technique. To optimize the planform shape, aerodynamic drag was minimized under various constraints given by the other disciplines. As a

Presented as Paper 98-0601 at the AIAA 36th Aerospace Sciences Meeting, Reno, NV, 12–15 January 1998; received 24 February 1998; revision received 22 April 1999; accepted for publication 22 April 1999. Copyright © 1999 by the American Institute of Aeronautics and Astronautics, Inc. All rights reserved.

*Graduate Student, Department of Aeronautics and Space Engineering; currently Design Engineer, Mail Code 455-8515, Aircraft Engineering Department, Nagoya Aerospace Systems, Mitsubishi Heavy Industries, Ltd., Nagoya 455-8515, Japan.

†Associate Professor, Department of Aeronautics and Space Engineering; s.obayashi@computer.org. Senior Member AIAA.

‡Professor, Department of Aeronautics and Space Engineering. Associate Fellow AIAA.

result, cross-disciplinary tradeoffs were built into the MDO model implicitly. One of the conclusions of Ref. 9, therefore, was that a highly sophisticated MDO model was needed to obtain realistic wing planform shapes.

A much simpler MDO model is desired in the present study to construct a preprocess for the inverse design. Such a model can be constructed by avoiding the built in cross-disciplinary tradeoffs. This means that each disciplinary objective should be treated independently. In such multi-objective optimization problems (MOPs), it is more natural to find a set of compromise solutions known as Pareto solutions than to find a single optimal solution corresponding to a particular tradeoff.

Conventional optimization techniques have to seek such Pareto solutions one by one, by changing weights in the utility functions. In contrast, genetic algorithms[10] (GAs) can search multiple optimums from a population of points in parallel. This feature is very attractive for solving MOPs and, thus, GAs have been extended to MOPs as multi-objective GAs (MOGAs).[11] General reviews for MOGAs can be found in Refs. 12 and 13. Reference 14 reported that the use of MOGAs, allowed the use of a simple MDO model to examine cross-disciplinary tradeoffs in the wing planform optimization. This approach will be adopted as the first preprocess in this study.

The second preprocess for the inverse design will be the target pressure optimization for the optimized wing planform. In this step, design objectives have to be translated into target pressure optimization. A good target pressure should yield elliptic loading, a straight isobar pattern, and low profile drag. However, these design objectives conflict with each other in general. For example, the elliptic loading may require a higher lift in the midspan region, which causes a shock wave and thus results in higher drag. Therefore, this optimization problem should be solved by the multiobjective optimizer as well.

Minimization of the profile drag was discussed as the chordwise pressure optimization in Refs. 7 and 8, as mentioned before. This problem also had various constraints, and Ref. 7 mentioned the difficulty in applying a standard optimization technique. In Ref. 8, GA was applied successfully because of its robustness. The same method is going to be extended to three dimensions to be used as the second preprocess in this study, by using MOGAs.

In this work, the transonic wing inverse design optimization system has been constructed by coupling two preprocessing optimizations to an inverse design method. First, a wing planform shape is designed by using the MDO system based on aerodynamic performance, structural strength and weight, and fuel storage. Second, a target pressure distribution is optimized to reduce the profile drag as well as to minimize the induced drag. The straight isobar pattern also will be enforced. Finally, the corresponding wing geometry can be obtained from existing inverse methods. A flowchart of the proposed design system is given in Fig. 1. A design result will be examined in the Results section.

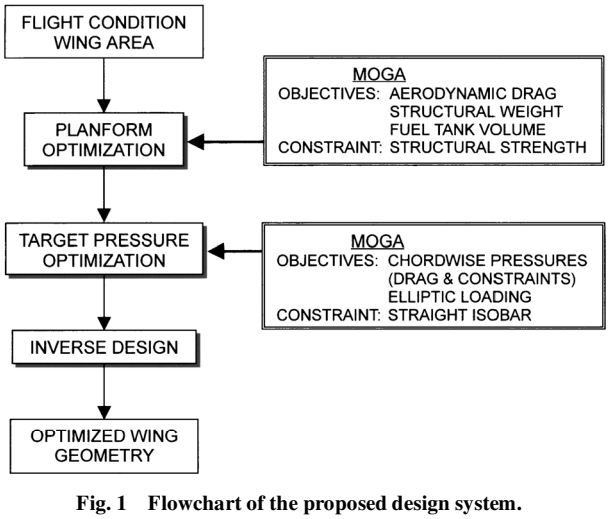

Fig. 1 Flowchart of the proposed design system.

MOGA

Conventional optimization algorithms assume that the optimization problem has (or can be reduced to) a single objective. Most engineering problems, however, require the simultaneous optimization of multiple, often competing, objectives. Solutions to MOPs are often computed by combining multiple objectivies into a single objective according to some utility function. In many cases, however, the utility function is not well known prior to the optimization process. The whole problem should then be treated with noncommensurable objectives. Multiobjective optimization seeks to optimize the components of a vector-valued objective function. Unlike single objective optimization, the solution to this problem is not a single point, but a family of points known as the Pareto-optimal set.

GAs are known to be robust optimization algorithms and have been enjoying increasing popularity in the field of numerical optimization in recent years. GAs are search algorithms based on the mechanics of natural selection and natural genetics. The basic procedures are shown in Fig. 2. One of the key features of GAs is that they search from a population of points, not a single point. Therefore, by maintaining a population of solutions, GAs can search for many Pareto-optimal solutions in parallel. This characteristic makes GAs very attractive for solving MOPs. As solvers for MOPs, the following two features are desired: 1) The solutions obtained are Pareto optimal. 2) They are uniformly sampled from the Pareto-optimal set. To achieve these with GAs, the ranking and niching techniques have been successfully combined into MOGAs.

Crossover and Mutation

In GAs, the natural parameter set of the optimization problem is coded as a finite-length string. Traditionally, GAs use binary numbers to represent such strings: A string has a finite length and each bit of a string can be either 0 or 1. For real-function optimization, however, it is more natural to use real numbers. The length of the real-number string corresponds to the number of design variables.

A simple crossover operator for real-number strings is the average crossover[15] that computes the arithmetic average of two real numbers provided by the mated pair. In this paper, a weighted average is used as

$$\text{Child1} = \text{ran1} \cdot \text{Parent1} + (1 - \text{ran1}) \cdot \text{Parent2}$$

$$\text{Child2} = (1 - \text{ran1}) \cdot \text{Parent1} + \text{ran1} \cdot \text{Parent2} \qquad (1)$$

where Child1 and Child2 and Parent1 and Parent2 are encoded design variables of the children (members of the new population) and parents (a mated pair of the old generation), respectively. The uniform random number ran1 in [0, 1] is regenerated for every design variable.

Mutation takes place at a probability of 20% (when a random number satisfies ran2 < 0.2) initially, and the rate is going to decline linearly during the evolution. Equations (1) will then be replaced by

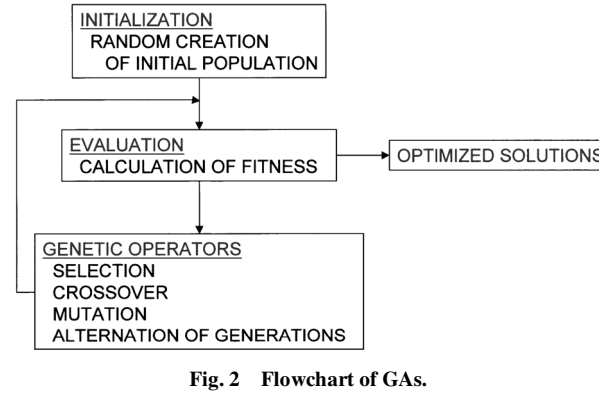

Fig. 2 Flowchart of GAs.

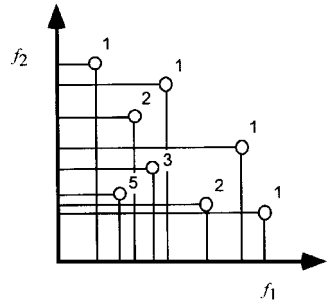

Fig. 3 Pareto ranking method.

$$\text{Child1} = \text{ran1} \cdot \text{Parent1} + (1 - \text{ran1}) \cdot \text{Parent2} + \text{m} \cdot (\text{ran3} - 0.5)$$

$$\text{Child2} = (1 - \text{ran1}) \cdot \text{Parent1} + \text{ran1} \cdot \text{Parent2} + \text{m} \cdot (\text{ran3} - 0.5) \tag{2}$$

where ran2 and ran3 are also uniform random numbers in [0, 1] and m determines the range of possible mutation.

Pareto Ranking

To search Pareto-optimal solutions by using MOGAs, the ranking selection method can be extended to identify the near-Pareto-optimal set within the population of GAs.[10,11] For single objective problems, the population can be sorted according to objective function values. The best individual receives rank 1, the second best receives rank 2, and so on. The fitness values are reassigned according to rank, for example, as an inverse of their rank values.

To consider MOPs, the following definitions are used: Suppose $\boldsymbol{x}_i$ and $\boldsymbol{x}_j$ are in the current population, and $\boldsymbol{f} = (f_1, f_2, \ldots, f_q)$ is the set of objective functions to be maximized.

1) Here $\boldsymbol{x}_i$ is said to be dominated by (or inferior to) $\boldsymbol{x}_j$, if $\boldsymbol{f}(\boldsymbol{x}_i)$ is partially less than $\boldsymbol{f}(\boldsymbol{x}_j)$, that is, $f_1(\boldsymbol{x}_i) \le f_1(\boldsymbol{x}_j) \wedge f_2(\boldsymbol{x}_i) \le f_2(\boldsymbol{x}_j) \wedge \cdots \wedge f_q(\boldsymbol{x}_i) \le f_q(\boldsymbol{x}_j)$ and $\boldsymbol{f}(\boldsymbol{x}_i) \neq \boldsymbol{f}(\boldsymbol{x}_j)$.

2) Here $\boldsymbol{x}_i$ is said to be nondominated if there does not exist any $\boldsymbol{x}_j$ in the population that dominates $\boldsymbol{x}_i$.

Nondominated solutions within the feasible region in the objective function space give the Pareto-optimal set. As an example, let us consider the following optimization: Maximize $f_1 = x$ and $f_2 = y$ subject to $x^2 + y^2 \le 1$ and $0 \le x,\ y \le 1$. The Pareto front of the this simple test case becomes a quarter arc of the circle $x^2 + y^2 = 1$ at $0 \le x,\ y \le 1$.

Consider an individual $\boldsymbol{x}_i$ at generation t (Fig. 3) that is dominated by p_i^t individuals in the current population. Following Ref. 11, its current position in the individuals' rank can be given by

$$\text{rank}(\boldsymbol{x}_i, t) = 1 + p_i^t$$

All nondominated individuals are assigned rank 1, as shown in Fig. 3 The fitness assignment according to rank can be done similarly to the single-objective case.

Niching

To sample Pareto-optimal solutions from the Pareto-optimal set uniformly, it is important to maintain genetic diversity. It is known that the genetic diversity of the population can be lost due to the stochastic selection process. This phenomenon is called the random genetic drift. To avoid such phenomena, the niching method has been introduced.[10]

The niching method penalizes the individuals crowded in a small niche by having them share the fitness as follows. A niche count of an individual is given by sum of a sharing function. The sharing function depends on the distance between individuals. If they are separated more than a specified distance, σ_{share}, the sharing function returns zero. If two individuals are closer than σ_{share}, the sharing function returns a higher value. If they are identical, the function returns the highest value of one. The original fitness value of the individual is then divided by the niche count. This scheme introduces new GA parameters, the niche size σ_{share}. The choice of σ_{share} has a significant impact on the performance of MOGAs.

The distance between individuals can be measured with respect to three types of metrics. A genotypic sharing measures the interchromosomal Hamming distance. A phenotypic sharing, on the other hand, measures the distance in the design space. Another type of phenotypic sharing measures the distance between the designs' objective function values. In MOGAs, the latter phenotypic sharing is usually preferred because we seek a global tradeoff surface in the objective function space.

Coevolutionary shared niching (CSN) is an alternate new niching method proposed in Ref. 16. The technique is loosely inspired by the economic model of monopolistic competition, in which businessmen locate themselves among geographically distributed populations, businessmen and customers, where individuals in each population seek to maximize their separate interests thereby creating appropriately spaced niches containing the most highly fit individuals.

The customer population may be viewed as a modification to the original sharing scheme, in which the sharing function and σ_{share} are replaced by requiring customers to share within the closest businessman's service area. In other words, a customer is supposed to be served by the nearest businessman. The number of customers a businessman serves becomes the niche count. Then, a customer's raw fitness is divided by the niche count similar to the original sharing scheme.

The evolution of the businessman population is conducted in a way that promotes the independent establishment of the most highly fit regions or niches in the search space. The businessman population is created by an imprint operator that carries the best of one population over the other. Simply stated, businessmen are chosen from the best of the customer population.

This model introduces a new GA parameter $d_{\min}$ that determines the minimum distance between the businessmen. It was found that $d_{\min}$ was easier to be tuned by the trial-and-error basis than by σ_{share}, and thus CNS was successfully applied to the following calculations.

Those who are interested in performance of these GA operators in a simple test case may refer to Refs. 16 and 17.

Wing Design System

Multidisciplinary Planform Design

As the first preprocess, this optimization problem determines the planform shape used in the inverse design. Although the planform design would require a careful study by itself, the present optimization is simplified so as to model only the basics of each discipline.

The present multiobjective optimization problem is described as follows: 1) minimize aerodynamic drag (mostly induced drag), 2) minimize wing weight, and 3) maximize fuel weight (tank volume) stored in the wing under the constraints 1) lift is to be equal to given aircraft maximum takeoff weight and 2) structural strength is to be greater than aerodynamic loads.[14]

The model aircraft considered here is a midsize regional aircraft, which was assumed to have a wing area of 525 ft^2, a total maximum takeoff weight of 45,000 lb at a cruise Mach number of 0.75, and a Reynolds number based on the root chord of 1.5×10^7. The original wing was taken from an existing wing: Its airfoil sections were supercritical, and its thickness and twist angle distributions were reduced toward the tip.

In this design stage, only two parameters are chosen as design variables: leading-edge sweep angle and taper ratio. A semispan length is calculated from the taper ratio and the given wing area. The number of design variables used was greatly reduced because any introduction of kinks to a wing for the regional aircraft would increase the manufacturing cost severely.

The objective functions and constraints are computed as follows. First, lift and drag are evaluated using a full potential flow solver called FLO27 (Ref. 18). In this preprocessing optimization, the wing area and the airfoil shape is fixed. Thus, the viscous drag can be regarded as nearly constant, and only a sum of induced and wave drag is needed. Therefore, the flow is assumed inviscid. Second, the wing weight is calculated, using an algebraic weight equation.[19] Third, the fuel weight is calculated directly from the tank volume given by the wing geometry. Finally, the structure is evaluated by using the model described in Ref. 9, where the wing box is modeled only for calculating skin thickness. Then the wing is treated as a thin-walled, single-cell monocoque beam to calculate stiffness. Flexibility of the wing is ignored.

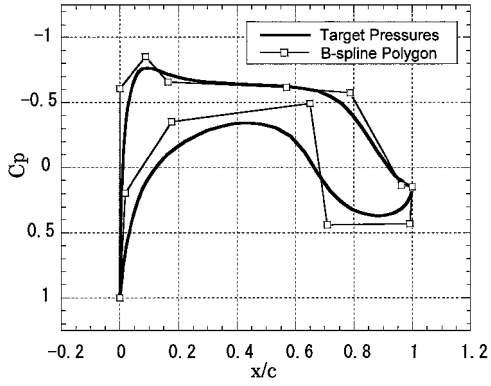

Fig. 4 B-spline polygon and corresponding pressure distribution.

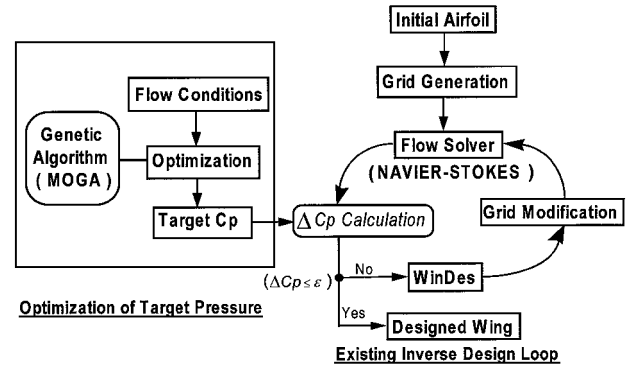

Fig. 5 Flowchart of the inverse design procedure.

The objective function values and constraint violations are now passed to the system-level optimizer, MOGA. When any constraint is violated, rank of the particular design is lowered by adding an integer according to the degree of violation.

Aerodynamic Design by Inverse Optimization

Here the design philosophy of target pressures for the inverse design is translated into MOPs. The aerodynamic design of a wing usually proceeds in two steps. First, the airfoil section at the midspan section is designed. This reduces the three-dimensional design problem into the two-dimensional one. Second, the spanwise variation of the airfoil sections is considered for the final wing design. The present objective functions are derived from those considerations.

Pressure Distribution for Airfoil

In Ref. 8, a GA has been applied to optimize target pressure distributions around airfoils for inverse design methods. An airfoil drag is minimized under constraints on lift, airfoil thickness, and other design principles. The same technique is adapted here.

Chordwise pressure distributions are parameterized by B-spline polygons and split into two curves, corresponding to the upper and lower surfaces of an airfoil. As shown in Fig. 4, seven points for lower surface and eight points for upper surface are used to define B-spline polygons, respectively.

The two-dimensional optimization problem is then defined as follows: Minimize drag coefficient C_d subject to 1) lift coefficient C_l = specified, 2) airfoil thickness to chord t/c = specified, and 3) additional constraints for chordwise pressure distribution, where C_d is evaluated by the Squire–Young relation and C_l and t/c can be estimated from surface pressure integrations. The specification of airfoil thickness can be done approximately in two dimensions, but not in three dimensions. Thus, it was dropped in the following three-dimensional optimization. Additional constraints are required to guarantee the existence of a solution of the aerodynamic inverse problem. They concern, for example, expansion at the leading edge, sonic plateau, rear loading, and so on (see Ref. 8 for details). The only new constraint introduced here is the Stratford pressure recovery[20] near the trailing edge.

Pressure Distribution for Wing

The design principles for a three-dimensional wing are essentially twofold. One is to preserve the two-dimensional performance as much as possible. This is easily achieved by the inverse method by specifying the same chordwise pressure distribution along the wing span. The resulting wing has the straight isobar pattern of pressure contours on the wing span.

The other is to minimize the induced drag, which is achieved by specifying a parabolic lift distribution in the spanwise direction when the structural constraint is imposed. The constraint in the total lift will specify a parabolic lift distribution uniquely. Thus, the objective function can be given by differences of the sectional lifts to the parabolic distribution at, for example, the seven spanwise sections.

The wing with the straight isobar pattern cannot have a parabolic lift distribution unless it has a parabolic planform. This means these two design objectives contradict each other in general. We overcome this problem by enforcing the isobar pattern only on the upper surface of the wing. The resulting straight isobar pattern of pressure on the upper surface of the wing is expected to produce the drag divergence at the same Mach number along the wing span, and thus the resulting drag-divergence Mach number of the wing will be similar to that of the wing that has a fully straight isobar pattern.

The three-dimensional optimization problem is now defined as follows: Minimize 1) the difference of the spanwise lift distribution to the parabolic distribution, 2) the two-dimensional drag coefficient C_d at each spanwise section, and 3) the penalty function based on the additional constraints for chordwise pressure distribution subject to the straight isobar pattern of pressure contours on the upper surface of the wing.

To generate a good initial population of feasible solutions, the two-dimensional GA was first run by using only the constraints. Then, the resulting chordwise pressure distribution was distributed to seven spanwise sections from the 10 to the 93% spanwise sections so as to give the parabolic lift distribution approximately. The population of 200 individuals was used as the initial population for the MOGA. Because the flow calculation required in this step is only the boundary-layer integration for the Squire–Young relation, the entire process runs easily on a regular workstation or personal computer. During the evolution, the pressure on the upper surface of the wing does not change very much because it is constrained not to change in the spanwise direction. Instead, the pressure on the lower surface of the wing is mainly modified to optimize the three preceding objectives.

Inverse Design

Once the present MOGA finds an optimum target pressure distribution, corresponding wing geometry can be obtained by an inverse design method. This design loop is shown in Fig. 5. Here the inverse design code WinDes[6] is used. WinDes uses the following iterative procedure. Suppose the initial geometry and surface pressure distribution obtained from any computational fluid dynamics (CFD) code are given. Then, pressure differences are calculated from the given initial and target pressure distributions. From these pressure differences, corresponding geometry corrections can be computed from the integral equations discretized at the panels on the wing planform. Improved geometry is then obtained from the initial geometry and the computed geometry corrections. Finally, the CFD code is used again to check how close the resulting pressure distribution is to the target distribution. If the differences are still large, the process will be iterated. In practice, 10–15 design cycles are sufficient to obtain the final geometry.

The inverse design code, Navier–Stokes code, and algebraic grid generator construct a nearly automated loop for the inverse design with reasonable computational requirements. These codes were implemented on a NEC SX-4 supercomputer at the Department of Aeronautics and Space Engineering, Tohoku University. The inverse design for one cycle required about 45 min of single CPU time. (Most of the time is used for the Navier–Stokes computation.)

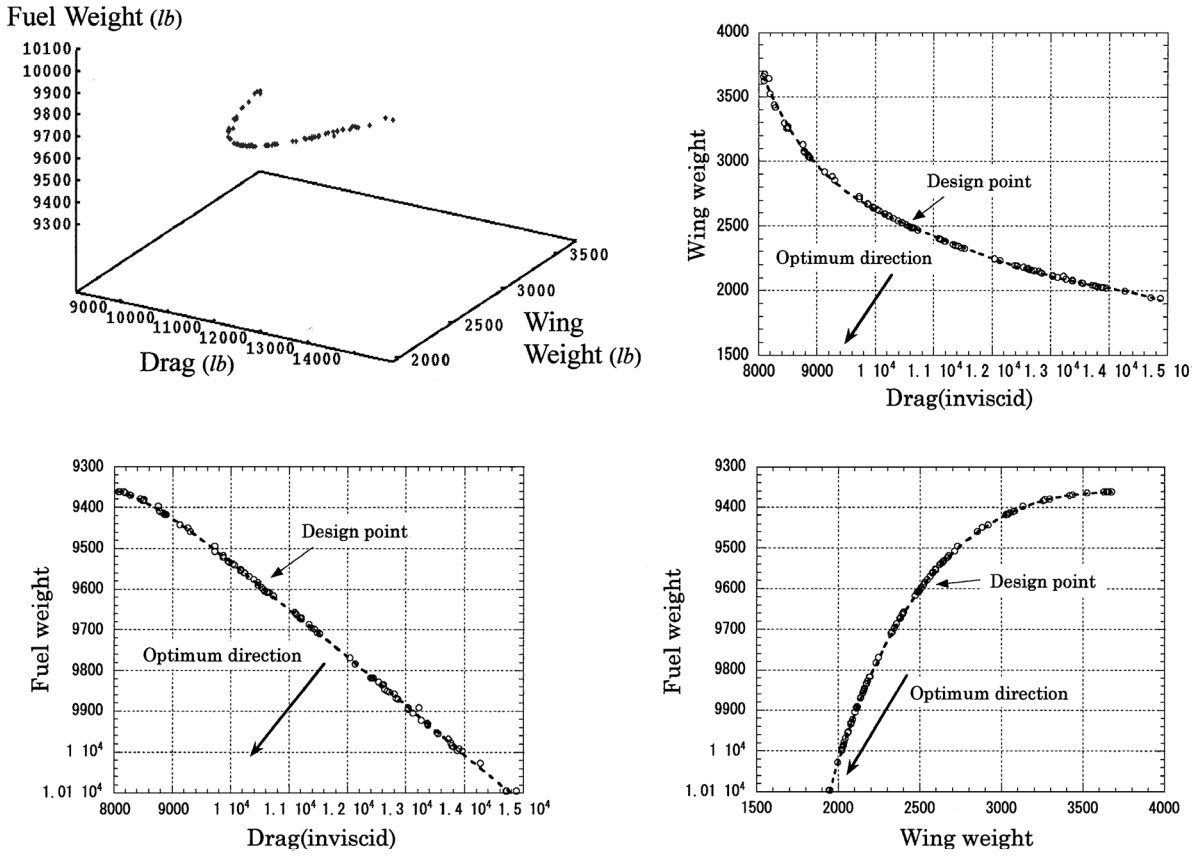

Fig. 6 Pareto solutions in the objective function domain.

Results

Multidisciplinary optimization of wing planform was performed with 100 individuals of population for the MOGA. Upper and lower limits of the design variables were defined as 5–20 deg for the sweep angle and 0.1–0.6 for the taper ratio. After 70 generations, almost all individuals were converged to the Pareto front. This corresponds to 8 h of single CPU time of an SX-4 computer. On the other hand, the inverse design required 15 cycles and it took roughly 11 h of CPU time. Because the computational cost of the wing planform optimization was comparable to that of the inverse design, no effort was taken to reduce the computational time further.

Because GA is a stochastic process, the present MOGA was run three times with different sets of initial populations. Figure 6 plots all individuals of the three populations in the objective function space after 70 generations. It is confirmed that the present MOGA consistently reproduce the same Pareto front every time, although the individuals on the Pareto front are different from population to population. The result also suggests a smaller population size may be used, but as mentioned before the possibility was not investigated here. (Our recent study shows that a MOGA using a population size of 64 works fine with 66 design variables for the wing definition.[21])

Figure 6 shows the locus of the Pareto solutions in the objective function space. All three axes are arranged so that the left lower corner becomes the desired point. The Pareto front, namely, the tradeoff surface, appears as a curve in the three-dimensional objective function space rather than as a surface. This is probably because only two design variables are used. In fact, the two-dimensional projections of the Pareto front to the drag to wing weight and drag to fuel weight planes show a very simple curve of tradeoffs. On the other hand, the projection to the wing weight to fuel weight plane does not show any tradeoff. Here the middle of the drag to wing weight tradeoff surface is chosen as a planform shape for the inverse design.

Figure 7 shows extreme Pareto solutions in the planform shape. Because the extreme Pareto solutions correspond to optimal solutions for each single objective, they can be used to judge the quality of Pareto solutions. The minimum drag wing has the smallest

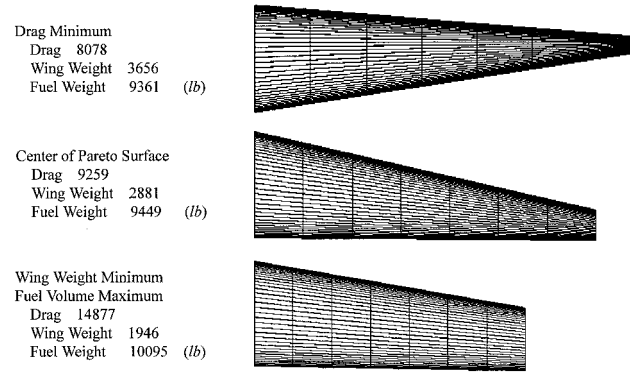

Fig. 7 Planform shapes of extreme Pareto solutions.

taper ratio among the feasible solutions, but slightly greater than the lower limit. Although the lowest taper ratio (the largest aspect ratio) in the design space can achieve the lowest drag, it also violates the structural constraint. Thus, this solution corresponds to the lowest possible taper ratio. The individual corresponding to the minimum wing weight and the maximum fuel weight has the same shape because the wing area is fixed in this optimization. These shapes have the maximum taper ratio. Therefore, the extreme Pareto solutions are found physically reasonable. The wing shape at the center of the Pareto surface has the most reasonable shape and can be considered as the best compromise between the multiple objectives here.

Next, the three-dimensional pressure distribution was optimized for the best compromise planform obtained, and then an inverse problem was solved. The parabolic lift distribution is monitored at seven locations from the 10 to the 93% span as indicated in Fig. 8. The inverse solver is used at the same spanwise locations for the geometry correction. For the Navier–Stokes analysis, the modification of wing geometry was linearly interpolated between those sections, and the twist angles of the designed wing at those sections

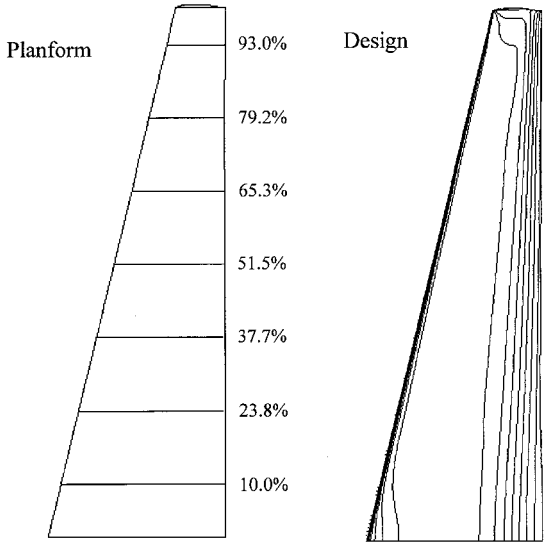

Fig. 8 Wing planform and computed pressure distribution on the designed wing.

are smoothed for simplicity of manufacturing. In the tip and root region, the airfoil sections were extrapolated from the interior sections, whereas the wing twist was linearly extrapolated. At the root section the fuselage is ignored, and the symmetry plane is assumed. It should be pointed out that the tip and root sections are usually designed by other means, and thus they are not treated by the inverse method.

The computational mesh for Navier–Stokes analysis has the C–O topology and contains $169 \times 49 \times 37$ grid points in the chordwise normal (to the surface) direction and spanwise directions, respectively. Although the grid size used was relatively small, it was considered sufficient for demonstration purposes. That was because 1) the wing planform was a simple tapered wing and 2) it was enough to predict a drag difference between different wings correctly. (If $C_{D_{\text{wing1}}} < C_{D_{\text{wing2}}}$ on the present grid, then $C_{D_{\text{wing1}}} < C_{D_{\text{wing2}}}$ on a grid refined doubly in every coordinate direction.)

Figure 8 shows the wing planform and the computed pressure contours on the upper surface of the wing designed by the inverse method based on the target pressure distribution optimized by the MOGA. Flow condition was set to the freestream Mach number of 0.75, the Reynolds number based on the root chord of 1.5×10^7, and an angle of attack of 0 deg. The resulting straight isobar pattern satisfies the first design principle of the wing well and, thus, indicates good performance at higher Mach numbers.

Figure 9 shows the target chordwise pressures obtained from the present MOGA, the resulting airfoil shapes of the wing obtained from WINDES, and the corresponding pressures computed by the Navier–Stokes solver. The target pressure shows sonic plateau, front and rear loadings, and Stratford pressure recovery. The upper surface pressures are exactly the same along the spanwise direction to produce the straight isobar pattern. It also confirms that the inverse problem is solved satisfactorily, although the front loading in the target pressure results in a small leading-edge radius in the present design.

Figure 10 shows the computed lift distribution of the designed wing in comparison to the parabolic distribution. The result is found to satisfy the second design principle of the wing, except at the root and tip regions where low and high sectional loadings are required, respectively, due to the straight isobars on the tapered wing.

As discussed in the Introduction, the optimality of the inverse design depends on physical properties of specified pressures. In this work, three-dimensional pressure distribution was constructed by distilling the design objectives of the transonic wing. Those objectives consist of sonic plateau, shock free, Stratford pressure recovery, parabolic spanwise loading, and straight isobar pattern. Figures 8–10 confirm that these objectives are materialized in the wing geometry designed by the inverse method.

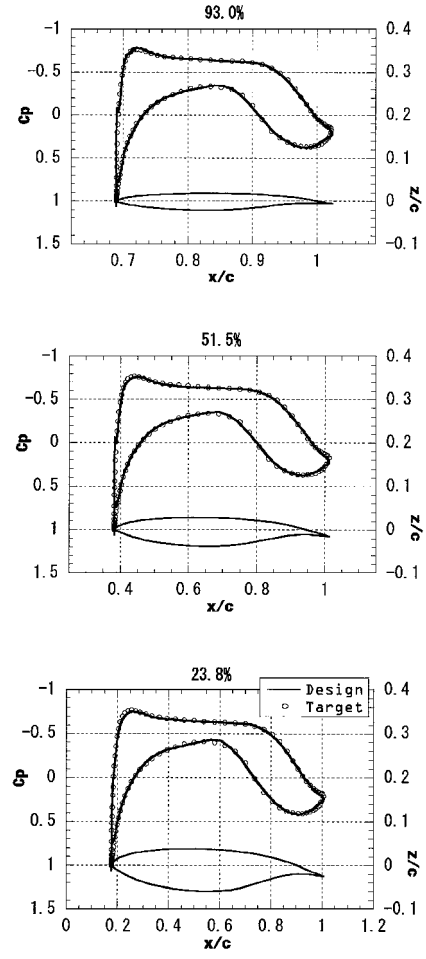

Fig. 9 Designed airfoil sections and corresponding chordwise pressure distributions.

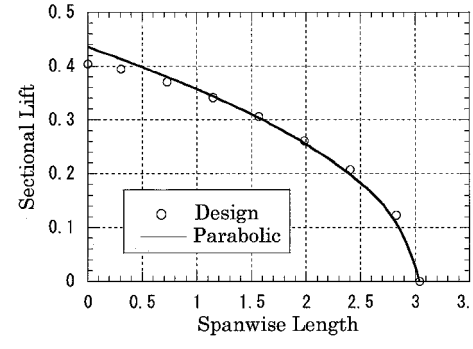

Fig. 10 Sectional lift distribution in the spanwise length.

Conclusion

An optimization system for an inverse design of transonic wings has been developed by using MOGAs based on the Pareto ranking method. First, planform shapes with minimum drag, minimum weight, and maximum fuel weight under constraints of lift and structural strength were sought by using the multidisciplinary model that consisted of the potential flow, algebraic weight, and wing-box structure equations. A wide variety of Pareto solutions were obtained, including a good compromise solution.

Second, target pressure optimization was performed for the planform obtained. The optimization problem was formulated to minimize the induced drag as well as to minimize the profile drag. The present design procedure also enforced the straight isobar pattern on the upper surface of the wing at the same time.

These two design optimization procedures were successfully applied to the inverse design of a transonic wing. The tradeoff information was given by the Pareto front, and the best compromise wing was able to be designed. The present approach will provide a practical automated design tool for the aircraft industry.

Acknowledgment

This work has been supported by Bombardier Aerospace, Toronto, Ontario, Canada.

References

[1]Gunzburger, M. D., "A Prehistory of Flow Control and Optimization," *Flow Control*, edited by M. D. Gunzburger, Springer–Verlag, New York, 1995, pp. 185–195.

[2]Reuther, J. J., Jameson, A., Alonso, J. J., Rimilinger, M. J., and Saunders, D., "Constrained Multipoint Aerodynamic Shape Optimization Using an Adjoint Formulation and Parallel Computers, Part 1," *Journal of Aircraft*, Vol. 36, No. 1, 1999, pp. 51–60.

[3]Newman, J. C., III, Taylor, A. C., III, Barnwell, R. W., Newman, P. A., and Hou, G. J.-W., "Overview of Sensitivity Analysis and Shape Optimization for Complex Aerodynamic Configurations," *Journal of Aircraft*, Vol. 36, No. 1, 1999, pp. 87–96.

[4]Borggaard, J. T., "On the Presence of Shocks in Domain Optimization of Euler Flows," *Flow Control*, edited by M. D. Gunzburger, Springer–Verlag, New York, 1995, pp. 35–48.

[5]Obayashi, S., and Tsukahara, T., "Comparison of Optimization Algorithms for Aerodynamic Shape Design," *AIAA Journal*, Vol. 35, No. 8, 1997, pp. 1413–1415.

[6]Takanashi, S., "Iterative Three-Dimensional Transonic Wing Design Using Integral Equations," *Journal of Aircraft*, Vol. 22, No. 8, 1985, pp. 216–222.

[7]Van den Dam, R. F., van Egmond, J. A., and Slooff, J. W., "Optimization of Target Pressure Distributions, Special Course on Inverse Methods for Airfoil Design for Aeronautical and Turbomachinery Applications," Rept. 780, AGARD, Nov. 1990, Ref. 3.

[8]Obayashi, S., and Takanashi, S., "Genetic Optimization of Target Pressure Distributions for Inverse Design Methods," *AIAA Journal*, Vol. 34, No. 5, 1996, pp. 881–886.

[9]Wakayama, S., and Kroo, I., "Subsonic Wing Planform Design Using Multidisciplinary Optimization," *Journal of Aircraft*, Vol. 32, No. 4, 1995, pp. 746–753.

[10]Goldberg, D. E., *Genetic Algorithms in Search, Optimization and Machine Learning*, Addison–Wesley, Reading, MA, 1989, pp. 1–23.

[11]Fonseca, C. M., and Fleming, P. J., "Genetic Algorithms for Multiobjective Optimization: Formulation, Discussion and Generalization," *Proceedings of the 5th International Conference on Genetic Algorithms*, edited by S. Forrest, Morgan Kaufmann, San Mateo, CA, 1993, pp. 416–423.

[12]Fonseca, C. M., and Fleming, P. J., "Multiobjective Optimization," *Handbook of Evolutionary Computation*, edited by T. Back, D. B. Fogel, and Z. Michalewicz, Inst. of Physics Publishing, Bristol, England, UK, and Oxford Univ. Press, New York, 1997, Sec. C4.5.

[13]Horn, J., "Multicriterion Decision Making," *Handbook of Evolutionary Computation*, edited by T. Back, D. B. Fogel, and Z. Michalewicz, Inst. of Physics Publishing, Bristol, England, UK, and Oxford Univ. Press, New York, 1997, Sec. F1.9.

[14]Obayashi, S., Yamaguchi, Y., and Nakamura, T., "Multiobjective Genetic Algorithm for Multidisciplinary Design of Transonic Wing Planform," *Journal of Aircraft*, Vol. 34, No. 5, 1997, pp. 690–693.

[15]Davis, L., *Handbook of Genetic Algorithms*, Van Nostrand Reinhold, New York, 1990.

[16]Goldberg, D. E., and Wang, L., "Adaptive Niching Via Coevolutionary Sharing," Illinois Genetic Algorithms Lab., IlliGAL Rept. 97007, Univ. of Illinois, Urbana, IL, 1997.

[17]Obayashi, S., Takahashi, S., and Takeguchi, Y., "Niching and Elitist Models for MOGAs," *Parallel Problem Solving from Nature—PPSN V*, Lecture Notes in Computer Science, Springer, Berlin, 1998, pp. 260–269.

[18]Jameson, A., and Caughey, D. A., "A Finite Volume Method For Transonic Potential Flow Calculations," AIAA Paper 77-677, Jan. 1977.

[19]Torenbeek, E., *Synthesis of Subsonic Airplane Design*, Kluwer, Dordrecht, The Netherlands, 1982, pp. 451–455.

[20]Liebeck, R. H., "Subsonic Airfoil Design," *Applied Computational Aerodynamics*, edited by P. A. Henne, AIAA, Washington, DC, 1990, pp. 133–165.

[21]Obayashi, S., Sasaki, D., and Takeguchi, Y., "Evolutionary Computation of Supersonic Wing Shape Optimization," *GECCO-1999: Proceedings of the Genetic and Evolutionary Computation Conference*, Vol. 2, Morgan Kaufmann, San Francisco, 1999, p. 1791.

A. Chattopadhyay
Associate Editor